The Plant Cell, Vol. 17, 1090–1104, April 2005, www.plantcell.org

Sites and Regulation of Auxin Biosynthesis in Arabidopsis Roots

Karin Ljung,[a] Anna K. Hull,[b] John Celenza,[c] Masashi Yamada,[d] Mark Estelle,[d] Jennifer Normanly,[e] and Göran Sandberg[a,1]

[a] Umeå Plant Science Center, Department of Forest Genetics and Plant Physiology, Swedish University of Agricultural Sciences, SE-901 83, Umeå, Sweden
[b] Center for Molecular Biotechnology, Fraunhofer USA, Newark, Delaware 19711
[c] Department of Biology, Boston University, Boston, Massachusetts 02215
[d] Department of Biology, Indiana University, Bloomington, Indiana 47405
[e] Department of Biochemistry and Molecular Biology, University of Massachusetts, Amherst, Massachusetts 01003

Auxin has been shown to be important for many aspects of root development, including initiation and emergence of lateral roots, patterning of the root apical meristem, gravitropism, and root elongation. Auxin biosynthesis occurs in both aerial portions of the plant and in roots; thus, the auxin required for root development could come from either source, or both. To monitor putative internal sites of auxin synthesis in the root, a method for measuring indole-3-acetic acid (IAA) biosynthesis with tissue resolution was developed. We monitored IAA synthesis in 0.5- to 2-mm sections of *Arabidopsis thaliana* roots and were able to identify an important auxin source in the meristematic region of the primary root tip as well as in the tips of emerged lateral roots. Lower but significant synthesis capacity was observed in tissues upward from the tip, showing that the root contains multiple auxin sources. Root-localized IAA synthesis was diminished in a *cyp79B2 cyp79B3* double knockout, suggesting an important role for Trp-dependent IAA synthesis pathways in the root. We present a model for how the primary root is supplied with auxin during early seedling development.

INTRODUCTION

The development of shoot and root tissues in plants is a highly coordinated process that requires extensive signaling between different tissues to integrate environmental cues with the plant's intrinsic developmental program. For example, leaf development occurs in concert with the continuous formation of new lateral roots, which increase the capacity of the plant to take up water and nutrients from the soil. Indole-3-acetic acid (IAA), one of the endogenous auxins in plants, is important for many aspects of root growth and development (Muday, 2001; Casimiro et al., 2003; Friml, 2003; Grebe, 2004). The aerial parts of the plant, especially the young developing leaves, are believed to function as an important source of IAA for the rest of the plant (Ljung et al., 2001). IAA derived from the shoot is transported acropetally in the root via the stele toward the root tip (Muday, 2001; Friml, 2003). A sharp auxin gradient has been observed in the *Arabidopsis thaliana* primary root, with high levels of IAA in the most apical millimeter of the root tip (Bhalerao et al., 2002). There is evidence that IAA accumulating in the root tip can be transported farther in a basipetal manner toward the root's elongation and differentiation zones, where it is essential for developmental processes such as cell elongation, gravitropism, and the initiation and development of lateral roots (Rashotte et al., 2000; Casimiro et al., 2001; Swarup et al., 2001; Bhalerao et al., 2002; Ottenschläger et al., 2003). These processes appear to be dependent on auxin transport via the influx and efflux carriers of the polar auxin transport (PAT) system, directing IAA to specific cell types of the root apex (Swarup et al., 2001; Friml et al., 2002a, 2002b; Benková et al., 2003). Efflux carriers, in turn, appear to be regulated in part by endogenous flavonoids (Peer et al., 2004).

We recently demonstrated that the root system is not entirely dependent on shoot-derived auxin (Bhalerao et al., 2002). We observed that the emergence of lateral root primordia (LRP) in very young Arabidopsis seedlings (4 to 7 d after germination [DAG]) was highly dependent on aerially derived auxin but that in older seedlings (7 to 10 DAG) LRP emergence was less dependent on auxin coming from the shoot. We also observed a 10-fold increase in IAA biosynthesis capacity in the root system between 3 and 10 DAG, indicating that the root system gains competence to synthesize IAA early in seedling development.

A better insight into the mechanisms regulating auxin biosynthesis in the root would increase our understanding of the role of auxin in a developmental context. The Arabidopsis root provides an excellent model system for developmental studies (Benfey and Scheres, 2000), but the small size and the low levels of auxin have made it difficult to analyze auxin levels, biosynthesis, and turnover in a truly tissue-specific manner. However,

[1] To whom correspondence should be addressed. E-mail goran.sandberg@genfys.slu.se; fax 46-90-786-8165.
The author responsible for distribution of materials integral to the findings presented in this article in accordance with the policy described in the Instructions for Authors (www.plantcell.org) is: Göran Sandberg (goran.sandberg@genfys.slu.se).
Article, publication date, and citation information can be found at www.plantcell.org/cgi/doi/10.1105/tpc.104.029272.

an analytical technique that makes it possible to analyze endogenous IAA levels in submilligram amounts of plant tissue is available (Edlund et al., 1995), and by improving this technology, we have measured the IAA concentration in very small sections of Arabidopsis roots (Swarup et al., 2001; Bhalerao et al., 2002). To be able to identify true sinks and sources of IAA in plants, it is equally important to analyze synthesis and turnover rates of IAA in these tissues. In this study, we describe a method that allows measurements of IAA biosynthesis in submilligram amounts of plant tissue, using the incorporation of deuterium from deuterium oxide (^2H_2O) and a very selective and sensitive analytical technique: selected reaction monitoring mass spectrometry (SRM-MS). This new approach made it possible for us to identify the sites of IAA synthesis in roots and to investigate the regulatory mechanisms that influence IAA synthesis and turnover. We demonstrate here that the entire root has IAA synthesis capacity and that the synthesis rates are particularly high in the primary root tip and in the tips of developing lateral roots. We observed a decrease in IAA synthesis rate after treatment with the IAA transport inhibitor naphthylphthalamic acid (NPA), suggesting that feedback regulation is one important mechanism regulating IAA synthesis in the root. Analysis of synthesis capacity in excised roots or under conditions in which PAT is inhibited by NPA indicates that a substantial part of the de novo synthesized IAA observed in the root is synthesized in the aerial parts of the plant and transported down to the root system. Thus, the root is dependent on several sources of IAA, both proximal and distal.

IAA biosynthetic pathways are still incompletely defined in plants. Two general types of IAA synthesis pathways can be distinguished by stable isotope labeling studies. In Trp-dependent IAA synthesis, IAA is derived from the metabolism of Trp, and in Trp-independent IAA synthesis, IAA is derived from a precursor to Trp (likely indole glycerol phosphate) in a pathway that bypasses Trp completely (Figure 1). Genes encoding Trp-independent pathway enzymes have yet to be identified; however, several genes and gene families encoding putative Trp-dependent pathway enzymes are known (Bartel et al., 2001; Ljung et al., 2002; Normanly et al., 2005). For several of these genes, expression analysis provides supporting evidence for Trp-dependent IAA synthesis in the root, including *ASA1* (for anthranilate synthase α) (Niyogi and Fink, 1992), *TSB1* (for Trp synthase β) (Pruitt and Last, 1993), *NIT1* to *NIT4* (for nitrilases 1 to 4) (Bartel and Fink, 1994; Hillebrand et al., 1998; Müller et al., 1998; Kutz et al., 2002), and *AtAO-1* (for a putative indole-3-acetaldehyde oxidase) (Sekimoto et al., 1998). Arabidopsis nitrilases have varying in vitro activities toward indole-3-acetonitrile (IAN) (Vorwerk et al., 2001), converting it to IAA, and the *NIT1* and *NIT4* genes exhibit strong expression in root tips (Bartel and Fink, 1994). The gene encoding *AtAO-1*, an aldehyde oxidase from Arabidopsis with in vitro specificity for indole-3-acetaldehyde, is predominantly expressed in roots and specifically upregulated in the auxin-accumulating *superroot1* (*sur1*) mutant (Sekimoto et al., 1998). *CYP79B2* and *CYP79B3* encode cytochrome P450 enzymes that convert Trp to indole-3-acetaldoxime (IAOx) (Hull et al., 2000; Mikkelsen et al., 2000) in a pathway that branches to either indole glucosinolates (IGs) or IAA. Here, we describe how levels and synthesis rates of IAA and IAN are altered in mutants involved in Trp-dependent IAA biosynthesis. Specifically, downregulation of IAA synthesis was observed in the *cyp79B2 cyp79B3* double mutant. The *CYP79B2* and *CYP79B3* genes were strongly expressed in the primary root meristem and in developing lateral roots, tissues that also show high IAA synthesis capacity.

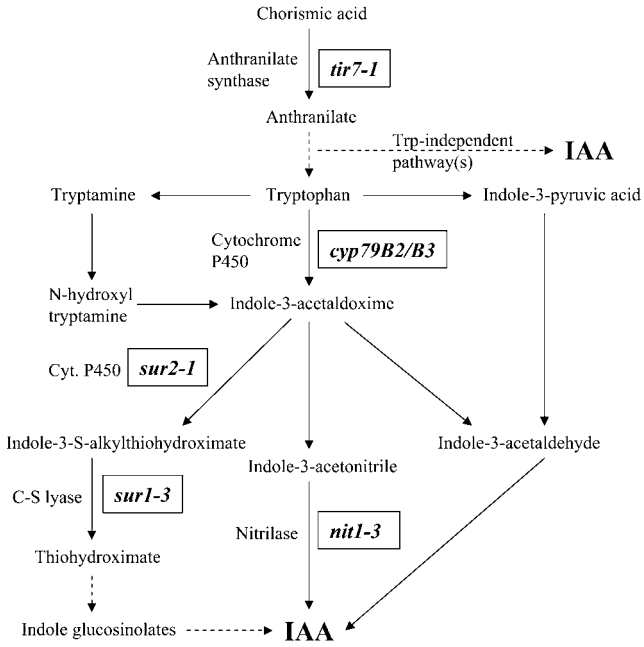

Figure 1. IAA Biosynthesis Pathways.

Putative pathways for Trp-dependent IAA synthesis in Arabidopsis. De novo biosynthesis of IAA and IAN was measured in root tips from different mutants in these pathways.

RESULTS

A Sensitive Method of Measuring de Novo IAA Biosynthesis with Tissue Resolution to 0.5-mm Root Sections

In vivo labeling with ^2H_2O has proven to be a useful tool for determining biosynthesis rates of a variety of metabolites (Boros et al., 2003). This tracer is especially useful when the synthesis pathways are not completely known, as in the case of IAA biosynthesis. Feedings are usually performed with medium containing 30% ^2H_2O, because higher concentrations might cause physiological effects such as growth retardation (Kushner et al., 1998). Studies of IAA metabolism have been performed in different plant species using this tracer (Cooney and Nonhebel, 1991; Bialek et al., 1992; Jensen and Bandurski, 1996; Ljung et al., 2001).

We previously determined IAA biosynthesis rates as a function of deuterium incorporation into IAA in different tissues of developing Arabidopsis seedlings using a method based on gas chromatography (GC)–high resolution selected ion monitoring (HR-SIM)–MS (Ljung et al., 2001; Bhalerao et al., 2002). These experiments indicated that the root has some capacity for de

novo IAA biosynthesis; however, in earlier work, the available technology did not provide sufficient resolution to define which part(s) of the root synthesized IAA. HR-SIM provided sufficient sensitivity to reliably quantify IAA biosynthesis rates when plant material in the range of hundreds of milligrams per sample was used for analysis, but with smaller amounts of tissue, chemical noise and low sensitivity render synthesis measurements impossible.

We have extensively used SRM-MS for quantification of endogenous levels of low-abundance plant hormones such as IAA, gibberellins, and cytokinins in different plant species (Edlund et al., 1995; Moritz and Olsen, 1995; Åstot et al., 2000). This scanning technique, which also has been used for measurements of cytokinin biosynthesis rates with LC-MS (Åstot et al., 2000), dramatically increases the sensitivity in quantitative analysis. It is based on the detection of daughter ions formed from the decomposition of metastable parent ions in the first field-free region of a double-focusing magnetic sector instrument (Gaskell and Millington, 1978; Thorne and Gaskell, 1985) and provides analytical sensitivity and selectivity comparable with, or in many cases superior to, corresponding analyses in the HR-SIM mode (Chapman, 1993; Moritz, 1996). For this technique to be useful for measurements of the incorporation of deuterium into the IAA molecule, deuterium incorporation should occur only in parts of the molecule that will become the metastable ion and not in the neutral moiety that is lost from the parent ion, because changes in mass resulting from the incorporation of deuterium are only monitored in the metastable ion. The molecule of the methylated and trimethylsilylated derivative of IAA (IAA-Me-TMS) fulfills this requirement, giving an abundant metastable ion (mass-to-charge ratio [m/z] 202) via the neutral loss of m/z 59 from the molecular parent ion (m/z 261) (Figure 2A). The incorporation of one to three deuterium atoms into the IAA molecule can then be monitored using the diagnostic metastable transitions m/z 262 to 203, m/z 263 to 204, and m/z 264 to 205 (Figure 2B). Corrections are made for the contribution of natural isotope abundances to m/z 203 to 205 by analyzing the same transitions from standard [$^{12}C_6$]IAA-Me-TMS. This is also necessary for the correction of small differences in instrument resolution between sample runs.

To determine whether any incorporation of deuterium into the IAA molecule could be of nonenzymatic origin, control samples were purified using HPLC and the IAA fraction was then subjected to strong alkaline conditions (Jensen and Bandurski, 1996) before GC-MS analysis of the isotopomer cluster. Comparison with untreated IAA fractions showed that no isotope exchange was observed after incubation of 2-week-old Arabidopsis seedlings with 30% ^2H_2O for 24 h (data not shown).

To compare the different analytical techniques, a deuterium labeling experiment was performed with 10-d-old Arabidopsis seedlings grown on agar plates. Intact seedlings or whole excised roots (roots incubated without aerial parts) were incubated for 12 or 24 h in liquid medium containing 30% ^2H_2O, and de novo IAA biosynthesis was measured by GC-MS on pooled root tissue using both the HR-SIM and SRM modes of detection. IAA biosynthetic rates were determined from the degree of incorporation of deuterium into the IAA molecule; as can be seen in Figure 2C, both methods gave almost the same rate of synthesis and similar standard deviations for all samples. In this experiment, the weight of the root samples was 30.1 ± 9.6 mg. Experiments were also performed to establish the smallest amount of tissue needed for accurate measurements of IAA biosynthesis in root tissue. Arabidopsis seedlings were incubated for 24 h with medium containing ^2H_2O, and different amounts of root tissue were collected and analyzed by GC-MS in both HR-SIM and SRM modes. Only SRM was sensitive and selective enough to provide accurate measurements of IAA biosynthesis in the low-milligram range of plant material. With this method, as little as 0.5 mg of root tissue was sufficient for accurate IAA biosynthesis measurements.

A Source of IAA Is Located within the Root Tip

Newly synthesized IAA was observed in root tissue after incubation of whole Arabidopsis seedlings in medium containing 30% ^2H_2O for 12 and 24 h (Figure 2C). Significant incorporation of deuterium into IAA was also detected in whole excised roots (Figure 2C, III 12 h and III 24 h), clearly demonstrating that the root has capacity for de novo IAA biosynthesis. To estimate the site(s) of IAA synthesis in the primary root, both intact Arabidopsis seedlings and whole excised roots were incubated for 24 h in medium containing 30% ^2H_2O, starting at 3 or 7 DAG. The apical 8 mm of each root was collected and divided into 2-mm sections, and IAA biosynthesis rates and IAA concentrations were analyzed in these sections by GC-SRM-MS (Figure 3). Root length and number of LRP was measured at 3, 4, 7, and 8 DAG (Table 1). For seedlings incubated from d 3 to 4 after germination, the 8-mm root section collected constituted the whole primary root. At this early stage of development, no stage V (Malamy and Benfey, 1997) or larger primordia were observed in the root, and meristematic tissue was present only in the primary root apex. In seedlings incubated from day 7 to day 8 after germination, lateral roots were developing at the basal part of the root, but in the apical 8 mm collected for IAA synthesis measurements, LRP were seen only at stages I to IV (Table 1). For these seedlings, the root tissue collected constituted 25 to 30% of the total primary root length (Figure 3E).

The highest rates of IAA biosynthesis were observed in roots from intact plants, in the most apical 2-mm section (Figures 3A and 3C, closed squares). Interestingly, a high rate of IAA synthesis was also observed in whole excised roots (Figures 3A and 3C, closed triangles). Lower but significant rates of IAA synthesis were observed in the region of the root that was farther away from the root apex, clearly demonstrating that all parts of the root have capacity for de novo IAA biosynthesis. Higher biosynthetic rates were found in all investigated parts of roots after incubation of intact plants (closed squares) compared with whole excised roots (closed triangles), probably reflecting the transport of newly synthesized IAA from aerial tissues down to the root system.

Intact seedlings were also incubated in medium containing both ^2H_2O and NPA to assess the effect of PAT on IAA biosynthesis. Treatment with NPA is believed to block PAT, trapping IAA in source tissues such as developing leaves. Clear effects of NPA treatment on the levels and distribution of newly synthesized IAA in the root were only observed in roots from intact seedlings incubated at 3 DAG (Figure 3A), with lower levels of

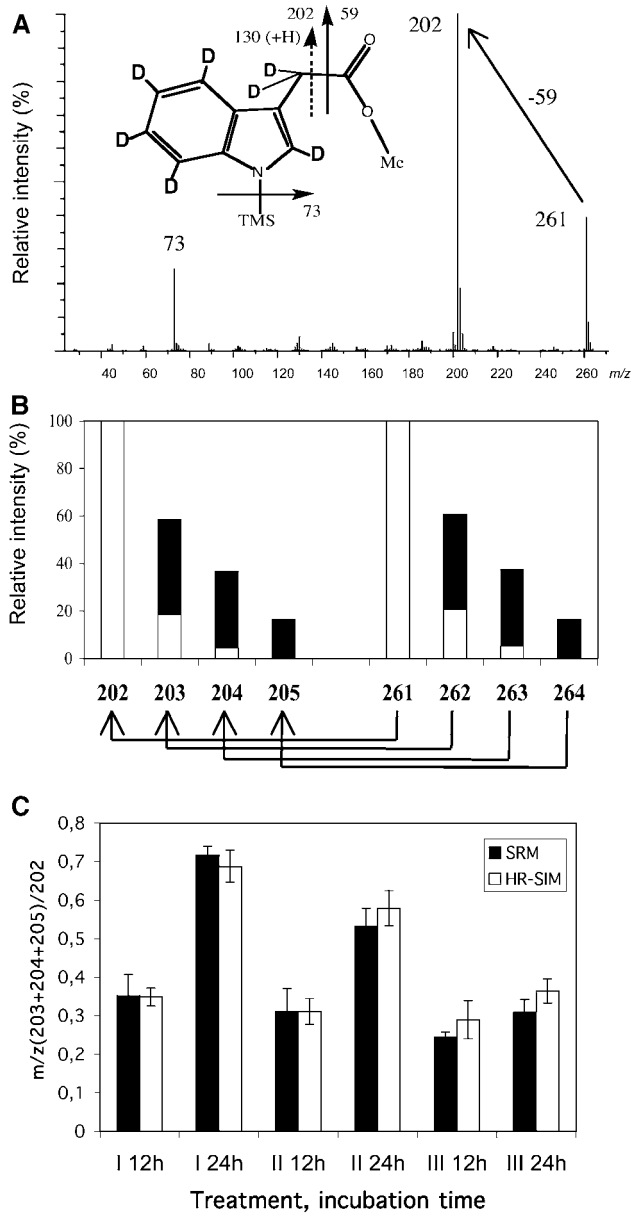

Figure 2. IAA Biosynthesis Measurements.

(A) Electron-impact mass spectrum and fragmentation pattern for IAA-Me-TMS. D indicates positions on the indole ring and side chain that can be labeled with deuterium.

(B) Mass isotopomer profiles for the molecular ion (m/z 261) and base peak (m/z 202) of IAA-Me-TMS. Natural isotope contribution (open bars) and deuterium labeling (closed bars) are indicated. Arrows indicate the metastable transitions that are monitored to calculate deuterium incorporation after feeding with ^2H_2O.

(C) Ten-day-old Arabidopsis seedlings were incubated for 12 and 24 h in medium containing ^2H_2O, and measurements of IAA biosynthesis rates were then performed on samples containing pooled root tissue from 10 seedlings. Three different experiments followed: (I) intact seedlings were incubated in medium containing 30% ^2H_2O; (II) intact seedlings were incubated in medium containing 30% ^2H_2O and 40 μM NPA; (III) excised roots were incubated in medium containing 30% ^2H_2O. Measurements were performed by SRM and HR-SIM-MS. Samples were measured in triplicate, and corrections were made for background and natural isotope abundances. Error bars indicate SD.

synthesized IAA in root sections from the NPA-treated seedlings (open squares) than controls (closed squares). However, the synthesis rate in the apical part of the root was not affected to the same extent as the more basal sections. Roots from intact seedlings incubated at 7 DAG did not show any significant alterations in the amount of newly synthesized IAA in the root after treatment with NPA (Figure 3C), suggesting that PAT is only of major importance for the supply of IAA to the root early in development.

Transport of IAA from the Shoot to the Root Is Important for the Formation of the IAA Gradient in the Root Tip

From the IAA synthesis data it was also possible to calculate the IAA concentration in the analyzed root sections. The incorporation of deuterium atoms into the IAA molecule changes the distribution of ions in the isotopomer cluster (m/z 202 to 205) of IAA-Me-TMS. After correction for natural isotope abundances, we calculated the total amount of IAA in the sample, combining the signals for unlabeled and labeled IAA. A sharp IAA concentration gradient was found in the root apex from intact plants, with the highest IAA levels in the most apical 2-mm section of the roots (Figures 3B and 3D). The IAA concentration gradient was reduced considerably in excised 8-d-old roots (Figure 3D, closed triangles) and was completely absent in excised 4-d-old roots (Figure 3B, closed triangles). In older seedlings, treatment with NPA caused an accumulation of IAA in the root tip (Figure 3D, open squares), in agreement with the findings of Casimiro et al. (2001).

The Highest IAA Synthesis Rate Was Observed in the Root Meristem

In an attempt to increase the spatial resolution of our analysis, the most apical 2 mm of the root tip was divided further into 0.5-mm sections after incubation of intact plants or excised roots in ^2H_2O-containing medium. IAA synthesis rates (Figure 4A) and levels (Figure 4B) were highest in the most apical 0.5 mm of the primary root tip, the region of the root tip that contains the root meristem.

Feedback Inhibition of IAA Synthesis Was Observed after NPA Treatment

GC-MS analysis of different sections of the primary root coming from seedlings grown in the presence of NPA shows that IAA accumulates in the root apex after NPA treatment in a concentration-dependent manner (Casimiro et al., 2001). The NPA treatment is believed to block basipetal transport of IAA in the root (Rashotte et al., 2000), thereby causing accumulation of IAA in the root apex, the part of the primary root that also has high IAA synthesis capacity (Figure 3). IAA synthesized in the root apex would then be trapped there, together with IAA transported

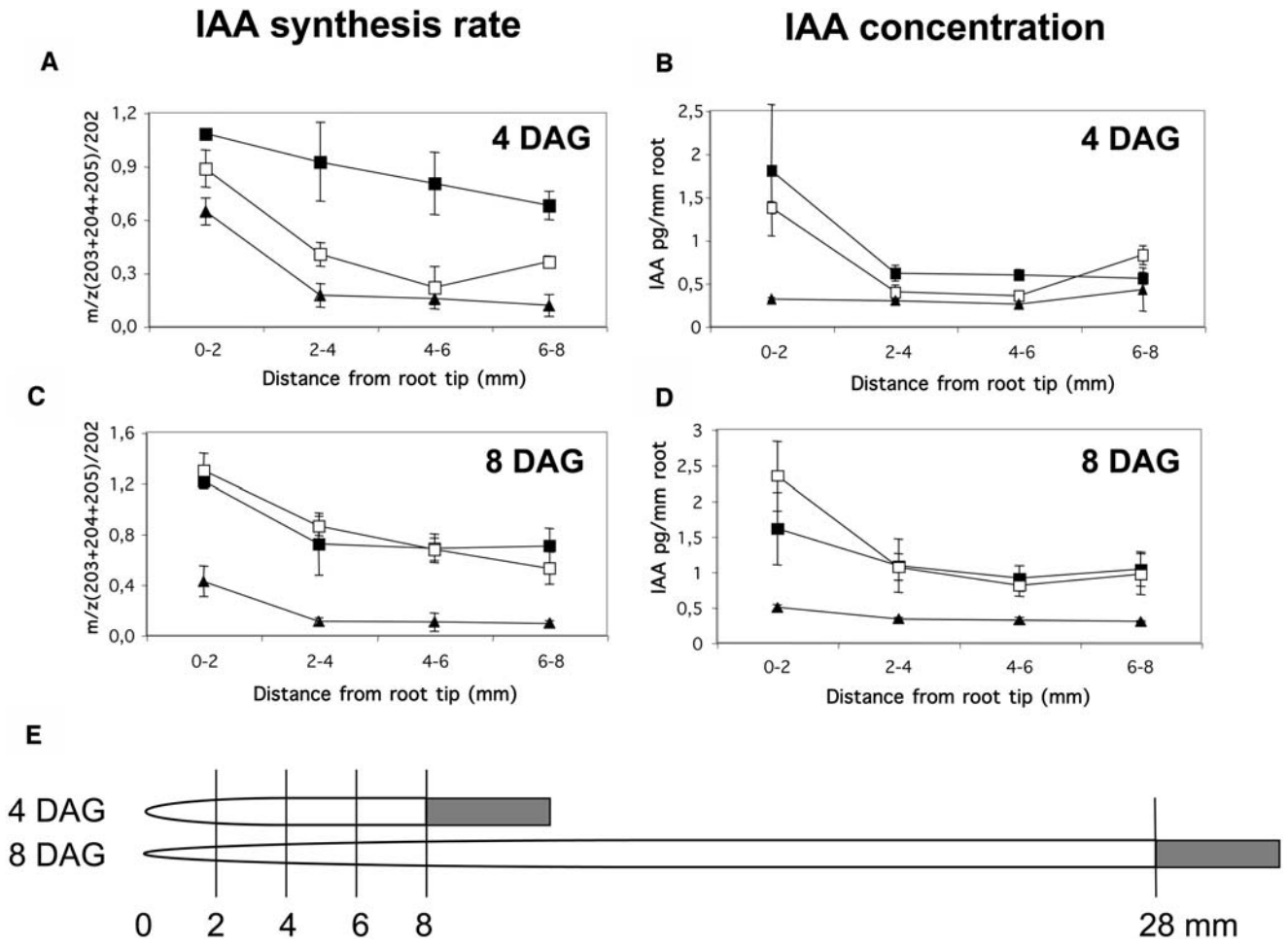

Figure 3. Distribution of IAA Biosynthesis and Concentration in the Arabidopsis Primary Root.

(A) to **(D)** De novo IAA biosynthesis rates (**[A]** and **[C]**) were measured in 2-mm root sections from Arabidopsis seedlings incubated for 24 h in medium containing ^2H_2O starting at 3 and 7 DAG. Endogenous IAA levels (**[B]** and **[D]**) in 2-mm root sections at 4 and 8 DAG were calculated from the data obtained in the IAA biosynthesis measurements by combining the corrected areas of the ions from deuterium-labeled IAA (m/z 203 to 205) with that of unlabeled IAA (m/z 202) after correcting for the natural abundance of stable isotopes. Error bars indicate SD. Experiments were performed with intact seedlings incubated in medium containing 30% ^2H_2O (closed squares), intact seedlings incubated in medium containing 30% ^2H_2O and 40 μM NPA (open squares), and excised roots incubated in medium containing 30% ^2H_2O (closed triangles).

(E) Root length and sampling positions for root tissue collected after feeding experiments performed 3 to 4 and 7 to 8 DAG.

to the root tip from the aerial part of the seedling. As a consequence of this IAA accumulation, different homeostatic mechanisms might be activated in the root apex.

An experiment was performed to investigate how NPA treatment affected the synthesis and concentration of IAA in the primary root. The NPA treatment was performed on excised roots to separate root-specific synthesis from IAA synthesis in the aerial part of the seedling. A clear feedback inhibition of IAA synthesis was observed in the root tip after incubation of 3-d-old excised seedling roots in medium containing ^2H_2O and 40 μM NPA to block PAT (Figure 4C). The same tendency was observed in the rest of the root, but the NPA treatment did not abolish IAA synthesis completely. This demonstrates that IAA synthesis is not only restricted to the root apex but that the whole root has IAA synthesis capacity. Interestingly, NPA treatment restored the IAA concentration gradient (Figure 4D), probably by restricting basipetal transport of newly synthesized IAA in the root tip.

Developing Lateral Roots Have the Capacity to Synthesize IAA

The fact that a weak IAA concentration gradient exists in the root tip coming from excised 8-d-old roots (Figure 3D, closed triangles) but not from excised 4-d-old roots (Figure 3B, closed triangles) suggests that the developing lateral roots can supply the primary root apex with auxin at a later developmental stage. IAA synthesis measurements performed on 8-mm sections of the primary root after incubation of intact seedlings and excised roots, starting at 7 DAG, showed that the synthesis rate (Figure 4E) and pool size (Figure 4F) increased in the basal part of the

Table 1. Root Development in Arabidopsis Seedlings

	DAG			
Root Development	3	4	7	8
Root length (mm)	5.1 ± 1.3	9.9 ± 1.8	24.5 ± 2.4	29.3 ± 3.2
Σ [LR + LRP ≥ V]	0	0.12 ± 0.52	4.4 ± 1.6	6.0 ± 1.7
	mm from root tip 8 DAG			
Σ [LR + LRP ≥ V]	0 to 8	8 to 16	16 to 24	24 to 32
	0	0.04 ± 0.2	1.6 ± 1.0	2.2 ± 1.0

Length of the primary root and number of developing lateral roots in Arabidopsis seedlings collected at different DAG. Lateral roots (LR) and lateral root primordia (LRP ≥ V) were counted and classified according to Malamy and Benfey (1997). Values (means ± SD) were calculated from measurements of 50 seedlings.

root after being lowest in the middle. To determine whether developing lateral roots have IAA synthesis capacity, whole roots were excised from 10-DAG seedlings and incubated in medium containing 30% ^2H_2O for 24 h, and the tips (2 mm) of developing lateral roots were collected for analysis. We observed a high synthesis rate in developing lateral roots [m/z (203 + 204 + 205)/202 = 0.83 ± 0.06], which was in the same range as the synthesis rate observed in 2-mm sections of the primary root tip from 4- and 7-d-old seedlings (Figures 3A and 3C).

IAA and IAN Synthesis Rates Are Changed in IAA Biosynthetic Mutant Lines

Plants rely upon multiple, genetically redundant IAA biosynthesis pathways (Bartel et al., 2001; Ljung et al., 2002; Normanly et al., 2005), although their use throughout the plant and over the course of the plant life cycle is incompletely defined. We used Arabidopsis mutants to examine three enzymatic steps in predicted IAA synthesis pathways for their contribution to the IAA pool in the root system. We also examined the cross talk between IG synthesis and IAA synthesis, using mutants that are defective in IG synthesis and that accumulate IAA. Synthesis rates for IAA and IAN (an intermediate in one of the Trp-dependent IAA synthesis pathways) were measured in 2-mm Arabidopsis root tip sections after incubation of intact seedlings and excised roots in medium containing ^2H_2O. Figure 1 describes putative IAA biosynthesis pathways in Arabidopsis and the different mutants used in this investigation.

The *transporter inhibitor response7-1* (*tir7-1*) mutant was originally identified in a screen for seedlings that are resistant to NPA (Ruegger et al., 1997). In addition to NPA resistance, the *tir7-1* mutation also confers a compressed root wave phenotype similar to that of the *trp5-1^{wvc1}* mutant, previously shown to be affected in the gene *ASA1*, which encodes the enzyme anthranilate synthase α (Niyogi and Fink, 1992; Rutherford et al., 1998). To determine whether *tir7-1* is an allele of *ASA1*, we crossed the mutant to the *trp5-1^{wvc1}* mutant. F1 seedlings had the same root wave phenotype as the parents, indicating that *tir7-1* is affected in the *ASA1* gene (data not shown). To confirm this, we determined the DNA sequence of *ASA1* from the *tir7-1* mutant. We identified a nucleotide substitution in the ninth exon of the gene resulting in the substitution of Gly-485 with an Asp residue.

Because anthranilate synthase is an early step in both Trp-dependent and Trp-independent IAA synthesis, we examined synthesis rates in the *tir7-1* mutant. Both IAA and IAN synthesis rates were significantly reduced in root tips isolated from intact seedlings of *tir7-1* compared with the wild type, whereas IAA and IAN synthesis rates in excised roots were the same as in the wild-type controls (Figure 5A). IAA levels in this mutant were substantially reduced in all root sections analyzed (Figure 6).

We also examined two known auxin-overproducing mutant lines, *sur2-1*, defective in the *CYP83B1* gene, which encodes an enzyme that converts IAOx to an indole-3-*S*-alkyl-thiohydroximate (Barlier et al., 2000; Bak et al., 2001), and *sur1-3*, reported to be defective in a C-S lyase that converts *S*-alkylthiohydroximates to thiohydroximates for all amino acid–derived aldoximes used in glucosinolate biosynthesis (Boerjan et al., 1995; Mikkelsen et al., 2004). We observed statistically significant increases in IAA synthesis rates for excised roots of *sur2-1* (Figure 5B) and *sur1-3* (Figure 5C) and a lower but still significant increase for *sur1-3* in roots from intact seedlings. Both mutants had significantly higher IAA concentrations than the wild type in all sections examined (Figure 6), which is consistent with their auxin-accumulating phenotypes (Boerjan et al., 1995; Barlier et al., 2000). IAN synthesis rates were diminished in both of these mutants compared with the wild type (Figures 5B and 5C).

Finally, we investigated two specific steps in predicted Trp-dependent IAA synthesis pathways. The conversion of Trp to IAOx is catalyzed by the cytochrome P450 enzymes CYP79B2 and CYP79B3 (Hull et al., 2000; Mikkelsen et al., 2000), and the *cyp79B2 cyp79B3* double knockout line carries T-DNA insertions in both of these genes. Another predicted IAA precursor, IAN, is converted to IAA by nitrilases (Bartel and Fink, 1994), and the *nit1-3* mutant is a null mutation in one of four Arabidopsis nitrilase genes, *NIT1*. The *cyp79B2 cyp79B3* double mutant exhibited a statistically significant decrease in IAA synthesis rate in the apical sections of excised roots (Figure 5D). IAA levels in root tips were not significantly reduced compared with the wild type (data not shown). The amount of IAN in these seedlings was too low to determine IAN synthesis rates, which is in agreement with the findings by Zhao et al. (2002), who observed lower IAA levels and very low IAN levels in the double mutant compared with the wild type. The *nit1-3* mutant did not show any significant changes in IAA synthesis rates (Figure 5E) or concentration (data not shown), either in intact seedlings or in excised roots. However, there was a significant increase in IAN synthesis in the apical section of excised roots, which could be attributed to the accumulation of newly synthesized IAN in the mutant as a result of greatly diminished turnover to IAA.

CYP79B2 and CYP79B3 Are Expressed in the Primary Root Meristem and at the Sites of Lateral Root Formation

Because the *cyp79B2 cyp79B3* double mutant showed a reduced IAA synthesis rate in roots, we wished to examine more closely the expression pattern of these two genes. A *CYP79B2*–β-glucuronidase (GUS) reporter construct has been shown

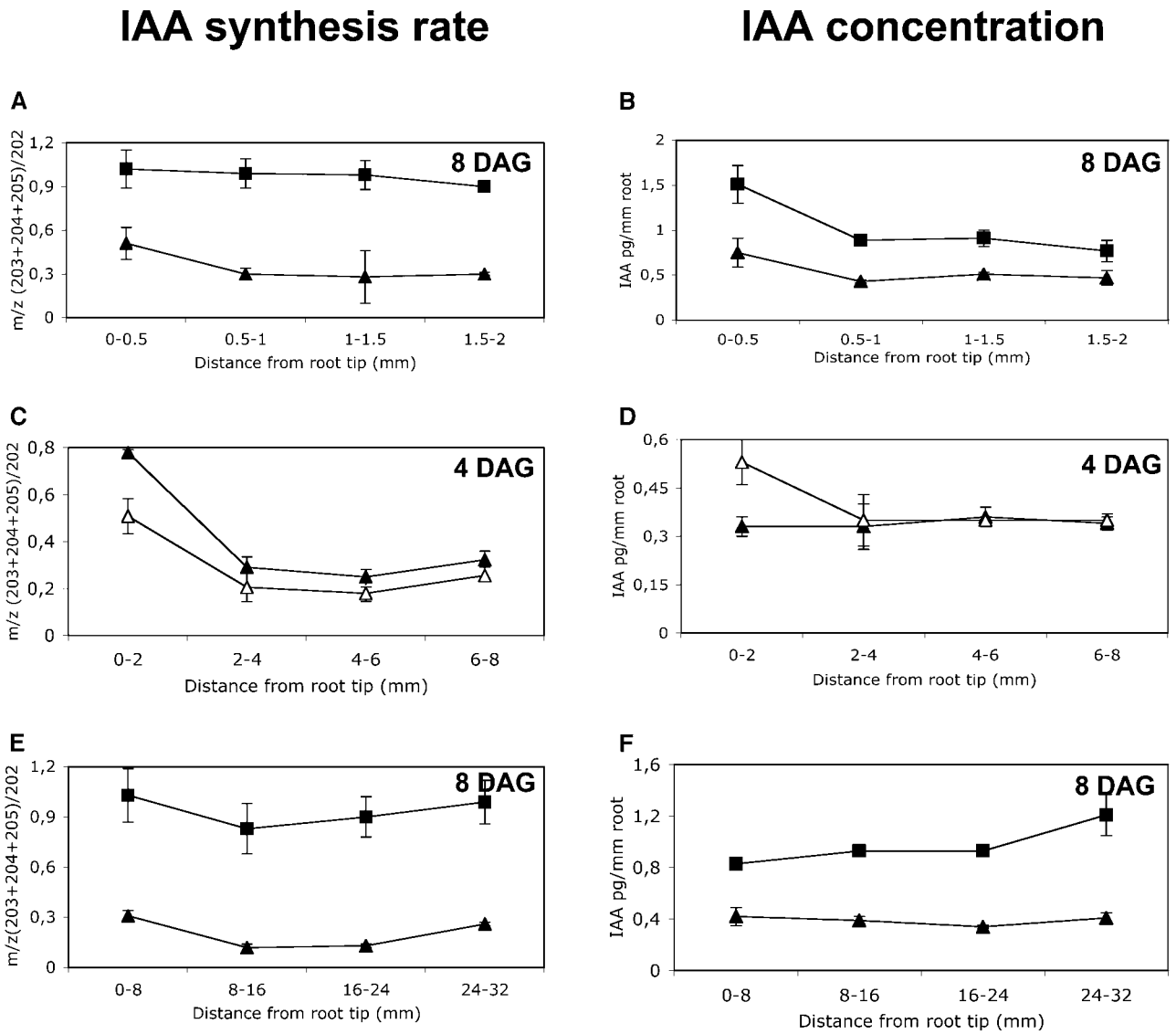

Figure 4. IAA Biosynthesis and Levels in Different Parts of the Arabidopsis Primary Root.

De novo IAA biosynthesis rate (**[A]**, **[C]**, and **[E]**) and IAA concentration (**[B]**, **[D]**, and **[F]**) were measured in different root sections after incubation of Arabidopsis seedlings in medium containing ^2H_2O. Error bars indicate SD.

(A) and **(B)** Intact seedlings (closed squares) and excised roots (closed triangles) were incubated in medium containing 30% ^2H_2O for 24 h starting at 7 DAG. Sections (0.5 mm) of the root tip were collected for analysis.

(C) and **(D)** Excised roots were incubated in medium containing 30% ^2H_2O (closed triangles) or 30% ^2H_2O and 40 μM NPA (open triangles) starting at 3 DAG. Sections (2 mm) of the root were collected for analysis.

(E) and **(F)** Intact seedlings (closed squares) and excised roots (closed triangles) were incubated in medium containing 30% ^2H_2O for 24 h starting at 7 DAG. Sections (8 mm) of the root were collected for analysis.

previously to be expressed in roots of older seedlings (Mikkelsen et al., 2000). To examine root expression in younger seedling and during lateral root formation, we created transgenic Arabidopsis lines carrying GUS reporters for *CYP79B2* and *CYP79B3*. The expression pattern in the root of the two constructs was similar, but subtle tissue-specific differences were observed. In the primary root meristem, *CYP79B2*-GUS appeared to be expressed in the outer layers of the meristem, whereas *CYP79B3*-GUS appeared to be expressed more centrally in the meristem (Figure 7A). Expression of both reporters was also observed at the sites of lateral root formation in the primary root (Figure 7B). *CYP79B2*-GUS was expressed in the primary root in the pericycle cell layers immediately underneath young LRP, and *CYP79B3*-GUS was expressed in cells of the primary root that surround LRP. Furthermore, *CYP79B3*-GUS expression extended into the base

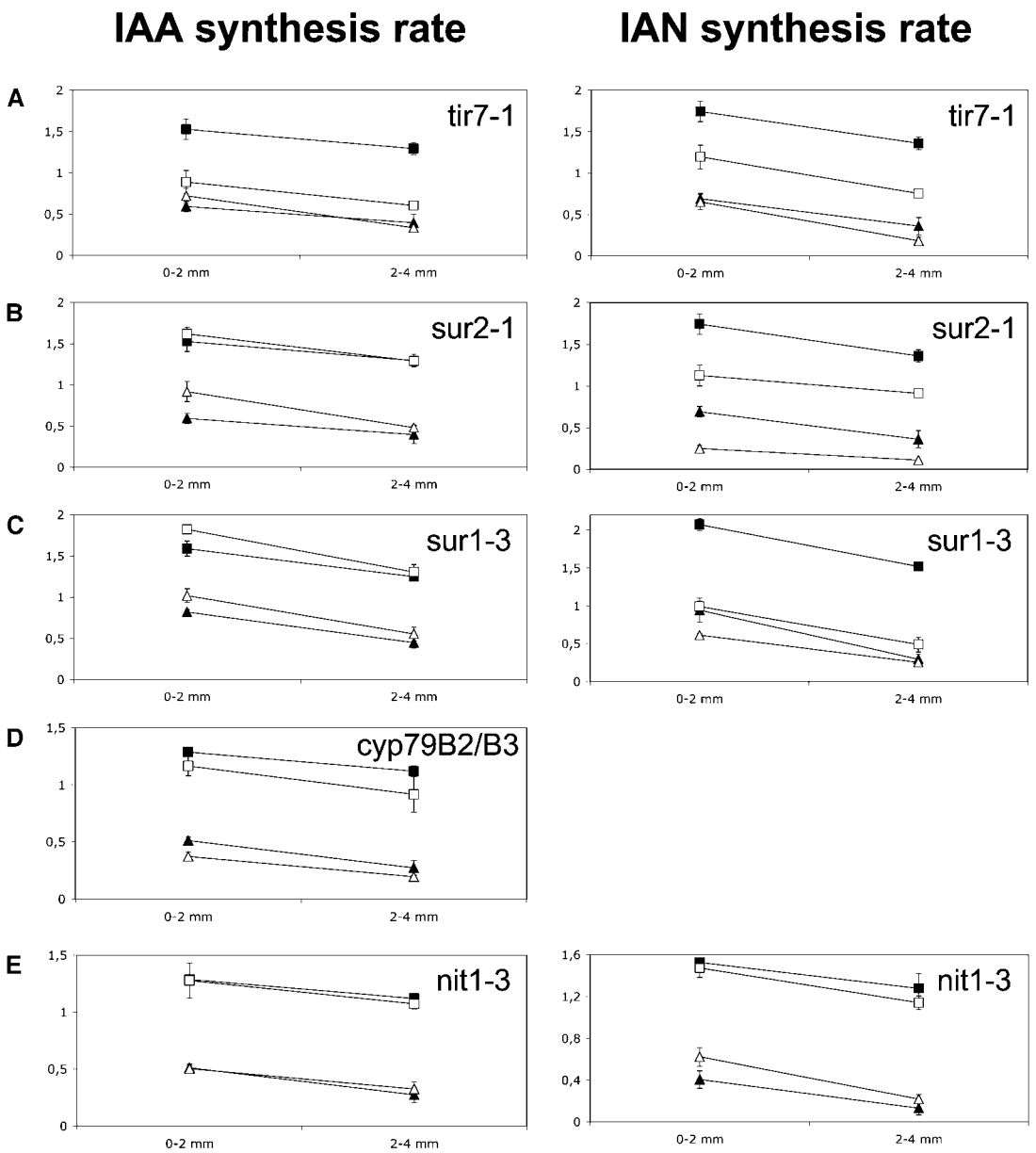

Figure 5. IAA and IAN Synthesis in Root Tips of IAA Biosynthesis Mutants.

IAA and IAN synthesis rates were measured in root tips from wild-type Columbia and the mutant lines *tir7-1* **(A)**, *sur2-1* **(B)**, *sur1-3* **(C)**, *cyp79B2 cyp79B3* **(D)**, and *nit1-3* **(E)**. Intact seedlings of the wild type (closed squares) and mutants (open squares) and excised roots of the wild type (closed triangles) and mutants (open triangles) were incubated in medium containing 30% ^2H_2O for 24 h starting at 7 DAG. The most apical 4-mm part of the primary root was collected in 2-mm sections. Error bars indicate SD.

of older emerging lateral roots, but *CYP79B2*-GUS expression did not (Figure 7C). In addition, *CYP79B3*-GUS was expressed in the new meristem of the lateral root, whereas *CYP79B2*-GUS was not expressed in the lateral root meristem until a later time (Figure 7C and data not shown). Treatment with 1 μM IAA for 24 h led to an increased lateral root induction (Figure 7D), with strong expression of both reporters at all sites of lateral root formation (but not in the rest of the primary root).

DISCUSSION

The experiments described here provide evidence that aerial tissues such as developing leaves are not the only source of the IAA needed for root development in Arabidopsis: there is also root-specific IAA biosynthesis. This physiochemical evidence shows that the primary root tip has high IAA synthesis capacity, suggesting a role for this newly synthesized IAA in root

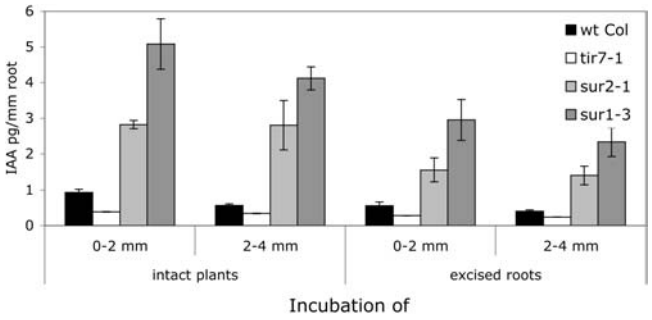

Figure 6. IAA Concentration in Root Tips of IAA Biosynthesis Mutants.

Endogenous IAA levels in 2-mm root sections were calculated from the data obtained in the IAA biosynthesis measurements (Figure 5) of different IAA synthesis mutants by combining the corrected areas of the ions from deuterium-labeled IAA (m/z 203 to 205) with that of unlabeled IAA (m/z 202). Error bars indicate SD. wt Col, wild-type Columbia.

development. Removal of the aerial parts of the seedling dramatically reduced the detected amount of synthesized IAA in the root tip, supporting the hypothesis that newly synthesized IAA is rapidly transported from shoot to root tissue, augmenting root-mediated IAA synthesis. We observed that the synthesis capacity in the root tip, although significant, was not high enough to maintain the basipetal IAA concentration gradient. Blocking PAT affected the amount of newly synthesized IAA detected in the root at 4 DAG but not at 8 DAG, showing that PAT from shoot to root tissue is more important early in seedling development. There is emerging evidence for another transport route for IAA from source to sink tissues besides PAT, suggesting that auxin can also be transported via the phloem. This hypothesis is based on the cellular localization of the auxin influx carrier AUX1, indicating that AUX1 can facilitate both phloem loading of auxin in leaves and phloem unloading in the root (Swarup et al., 2001; Marchant et al., 2002). Data from this study support this hypothesis, as does the observation that auxin transport from young, developing leaves to the root is not blocked in 10-d-old Arabidopsis seedlings treated with NPA (Ljung et al., 2001). The existence of more than one transport route to the root system of IAA complicates investigations of auxin transport, and the results from earlier experiments performed using PAT inhibitors might need to be reconsidered. Our experiments provide physicochemical evidence supporting the proposed phloem-mediated auxin transport.

IAA synthesis rates and levels in excised roots were substantially less than in sections from intact seedlings, confirming that the aerial parts of the plant function as a major source of IAA for the root system, and transport of IAA to the root apex is needed for the formation of the IAA gradient in the root tip. Analysis of root tips from intact seedlings demonstrates that the IAA gradient is already established at 4 DAG, in agreement with earlier reports (Bhalerao et al., 2002). The IAA concentration gradient was greatly diminished or absent in excised roots, although IAA biosynthesis was still fully active in the root apex. This finding suggests that two separate pools of IAA exist in the root apex, one transported from the shoot and one synthesized in the root apex. By removing the shoot, the root tip becomes deprived of IAA coming from aerial tissues, but basipetal transport of IAA is likely to transport IAA away from the source in the root tip to potential sinks located upward from the root apex. This would explain the disappearance of the gradient, without affecting the rate of IAA synthesized in the root tip. Further support for this model comes from previous work demonstrating that applied [^{3}H]IAA is transported at least 5 to 7 mm away from the root tip by basipetal transport (Rashotte et al., 2000).

The most apical 2 mm of the root tip, which showed strong IAA synthesis activity in this study, is a region of the root that includes a range of tissue types, such as the root cap, the root meristem, the elongation zone, and the differentiation zone where lateral root formation is initiated (Schiefelbein and Benfey, 1994; Dolan and Davies, 2004). By increasing the resolution of IAA synthesis measurements in roots, we observed the highest synthesis rate and level in the most apical 0.5 mm part of the root tip, containing the meristem. The primary root meristem has many cells undergoing rapid cell division (Beeckman et al., 2001; Birnbaum et al., 2003). It has also been observed (van der Weele et al., 2003) that the root tip contains two distinct zones with constant elongation rates, lower in the meristematic zone (0 to 0.5 mm from the tip) and much higher in the elongation zone (0.5 to 1.2 mm from the tip). In the differentiation zone, the growth rate decreases to zero. The role for locally synthesized IAA in different developmental processes in the root apex has yet to be investigated, but it might be important for the organization of the root meristem, initiation of LRP, and cell elongation. In developing tobacco leaves, high IAA levels were also found to be associated with parts of the leaf undergoing rapid cell division, and in Arabidopsis seedlings, the youngest leaves showed the highest IAA biosynthesis rates and IAA levels of all tissues examined (Ljung et al., 2001).

We previously demonstrated that the root system gains competence to synthesize IAA early in seedling development (Bhalerao et al., 2002), making the root less dependent on auxin coming from the shoot at 10 DAG compared with 3 DAG. The facts that a weak IAA concentration gradient exists in 8-d-old excised root tips, and that there is an increase in IAA synthesis rate in the part of the root where lateral roots are emerging, suggest that developing lateral roots can supply the primary root apex with auxin at later developmental stages. This was confirmed by IAA synthesis measurements in excised roots, showing that the tips of lateral roots have high IAA synthesis capacity. Laskowski et al. (1995) observed that LRP become independent of exogenous IAA for growth when they are approximately three to five cell layers thick (stages III to V [Malamy and Benfey, 1997]), a developmental stage at which they form a functional meristem. Our results indicate that this might be the stage at which IAA synthesis is initiated in developing lateral roots.

Feedback inhibition of IAA synthesis was observed after treatment of excised roots with NPA to block PAT. This has also been observed in developing leaves and cotyledons after treatment of 10-d-old Arabidopsis seedlings with NPA (Ljung et al., 2001). Feedback inhibition is a homeostatic mechanism that provides the root with a way to adjust root-specific IAA synthesis in concert with the flow of IAA coming from the shoot and the basipetal transport away from the root apex. Other IAA

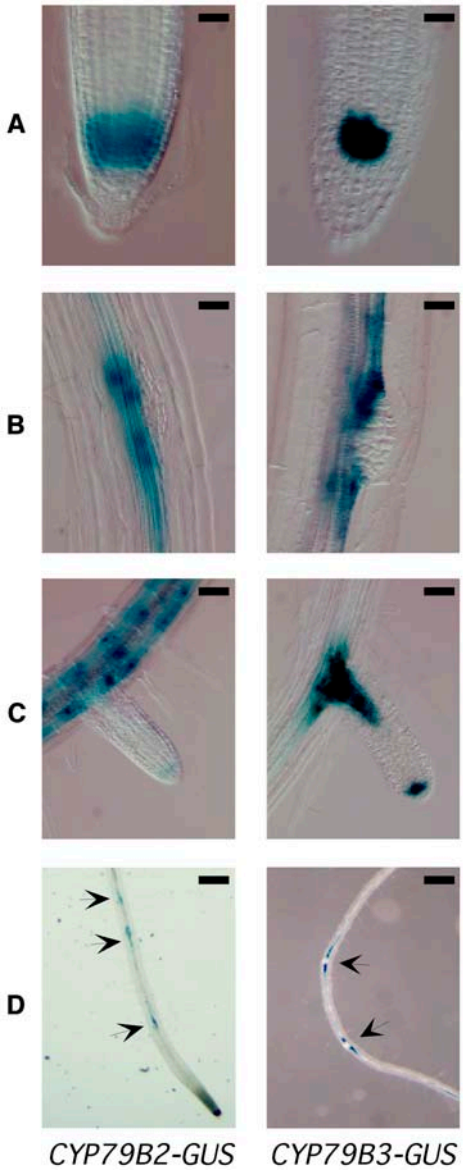

Figure 7. *CYP79B2-GUS* and *CYP79B3-GUS* Reporter Expression in Arabidopsis Roots.

CYP79B2-GUS transgenic plants are shown at left, and *CYP79B3-GUS* transgenic plants are shown at right. *CYP79B2-GUS* plants were stained with X-Gluc for 1 h, and *CYP79B3-GUS* plants were stained for 18 h.
(A) to **(C)** Expression patterns of *CYP79B2* and *CYP79B3* in the primary root tip **(A)**, sites of lateral root formation **(B)**, and developing lateral roots **(C)** of 7-DAG seedlings.
(D) The primary root after treatment with 1 μM IAA for 24 h at 7 DAG, showing expression at all sites of lateral root formation (arrows) but not in the rest of the primary root.
Bars = 25 μm in **(A)** and **(B)**, 50 μm in **(C)**, and 250 μm in **(D)**.

homeostatic mechanisms in the root, such as catabolism and conjugation, also might be important and need to be investigated.

As can be seen in the model presented in Figure 8, the most important sources of IAA for the developing root are transport of de novo synthesized IAA from aerial parts of the plant to the root and local synthesis in the primary and lateral root tips. IAA can then be transported acropetally within the root stele or basipetally from the root apex to other tissues within the root tip (Casimiro et al., 2003). Significant IAA synthesis also occurs in nonmeristematic parts of the root, indicating that there is a basal IAA synthesis capacity in all parts of the root system. It is not known if and how this IAA is transported within the root or if it acts locally at the site of synthesis. A putative transport route of IAA from the root stele to other parts of the primary root is also indicated.

Figure 1 shows IAA biosynthesis pathways that have been postulated for Arabidopsis. The Trp-independent pathway is believed to branch off between anthranilate and Trp, but no genes for this pathway have been identified to date. The *tir7-1* mutant, defective in the *ASA1* gene encoding anthranilate synthase α1, was used as a control in our study, because this

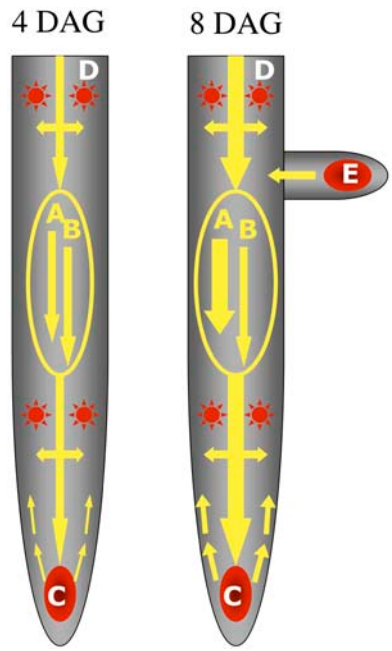

Figure 8. Model Showing How Different Sources Supply the Root with Auxin during Early Seedling Development.

Sources (red) and transport (yellow) of de novo synthesized IAA in the root system of Arabidopsis. At 4 DAG, auxin produced in the aerial part of the seedling is transported to the root via two routes of equal importance: phloem-mediated transport (A) and polar transport (B). At 8 DAG, the phloem-mediated transport is relatively more important than the polar transport. Already early in root development, two internal sources are established, one specifically localized to the outermost 0.5 mm of the root (C), and one representing all tissues upward from the root tip with low but important synthesis capacity (D). In the later stages of development, all emerging lateral roots gain synthesis capacity (E) and will be important contributors to the auxin pool in the root system.

mutation would affect both the Trp-dependent and Trp-independent pathways. Indeed, both IAA and IAN synthesis rates and IAA concentration were significantly lower in *tir7-1* root tips compared with wild-type root tips. The observation that IAA and IAN synthesis rates in excised roots of *tir7-1* were not significantly different from those of the wild type implies that the *tir7-1* defect has less impact on root-specific synthesis than on synthesis in the aerial portion of the seedling. Although the effect of the *tir7-1* mutation on *ASA1* function has not been determined directly, the mutation is likely to be a strong hypomorph or null. The affected residue, G485 is conserved among all anthranilate synthase α subunits and lies in a region of the protein that has been shown to be essential for enzyme activity (Bauerle et al., 1987). Replacement of this residue with Asp is likely to have a major effect on the function of the enzyme. In addition, the phenotype of *tir7-1* is very similar to that of *trp5-1*^{wvc1}. This mutation is caused by a T-DNA insertion in the fourth intron of the gene, thus preventing the synthesis of an intact *ASA1* transcript (Rutherford et al., 1998).

The known auxin overproducers *sur1-3* and *sur2-1* were used as tools to study the effect of increased flux through the IAA synthesis pathways. Both mutants showed higher IAA synthesis rates compared with the wild type, and they also had significantly higher IAA concentrations in all root sections examined, which is consistent with their auxin-accumulating phenotypes (Boerjan et al., 1995; Barlier et al., 2000). We did not measure the IAN concentration in these experiments, but previous work with *sur2-1* revealed a slight decrease in IAN level in this mutant (Barlier et al., 2000). *SUR2* is strongly expressed in roots (Mizutani et al., 1998) and encodes the enzyme CYP83B1, which catalyzes the first committed step in IG synthesis from IAOx. Defects in the conversion of IAOx would result in an accumulation of this compound and a shift to conversion of IAOx to IAA. The *SUR1* gene is believed to encode a C-S lyase that acts downstream of *SUR2* in IG synthesis. The *sur1-3* mutation would likely accumulate IAOx and/or divert this branch point compound to IAA synthesis. IAA synthesis activity in excised roots was higher in these mutants than in the wild type, consistent with the use of Trp-dependent IAA synthesis pathways in the root. IAOx conversion to IAA is presumed to go through an IAN intermediate, so we measured IAN synthesis in both *sur2-1* and *sur1-3*. We observed lower IAN synthesis rates in both mutants, suggesting either very rapid turnover of IAN to IAA or an alternative route to IAA from IAOx (Figure 1). Lower IAN synthesis rates in the *sur* mutants can also be explained by diminished IG levels, as they are predicted precursors to IAN. Indeed, IGs in *sur2* (*cyp83B1*) are reduced by ~50 to 60% (Bak et al., 2001), and *sur1* (heterozygote) apparently cannot synthesize any glucosinolates (Mikkelsen et al., 2004).

We also observed a significant decrease in IAA synthesis rate in excised roots of the *cyp79B2 cyp79B3* double mutant. This finding is consistent with previous work with this mutant in which IAA levels were slightly but significantly reduced in whole seedlings (Zhao et al., 2002). The observation that IAA synthesis is only reduced and not abolished completely in this mutant despite the fact that IAN levels are very low suggests other routes of IAA synthesis that do not involve either IAN or IAOx. However, the root-specific localization of CYP79B2 and CYP79B3 reporter constructs, combined with the fact that the only statistically significant decrease in IAA synthesis was observed in the apical section of excised roots in our study, indicates that these genes are involved in root-specific IAA synthesis.

The root tip–specific expression of *CYP79B2* and *CYP79B3* has been confirmed independently using global expression analysis of dissected root tissues and was found to overlap with the expression of other genes believed to be involved in IAA synthesis (Birnbaum et al., 2003). For example, *ASA1*, *ASA2*, and *ASB2* (anthranilate synthase β) had similar root tip expression patterns to *CYP79B2* and *CYP79B3* (Birnbaum et al., 2003). In addition, earlier studies found that expression of *TSB1* and *ASA1* is high in Arabidopsis root tips (Niyogi, 1993; Pruitt and Last, 1993). Furthermore, we recently found that dominant mutations in the *Altered Tryptophan Regulation1* (*ATR1*) gene, which encodes a Myb transcription factor, cause increased expression of *CYP79B2*, *CYP79B3*, and Trp biosynthetic genes and a concomitant increase in IAA levels (Bender and Fink, 1998; Smolen and Bender, 2002; Celenza et al., 2005).

A role for nitrilases in IAA synthesis is less clear; the nitrilase genes *NIT1* and *NIT4* are strongly expressed in Arabidopsis root tips, and *NIT1* is expressed at sites of LRP formation (Bartel and Fink, 1994; Müller et al., 1998), whereas *NIT3* is upregulated in root tips of sulfur-deprived plants (Kutz et al., 2002). However, the *nit1-3* mutant exhibited IAA synthesis rates and levels similar to those of the wild type in all sections examined, which does not support a significant role for *NIT1* in IAA synthesis. This finding is consistent with earlier analysis of this mutant, in which IAA levels in whole seedlings were similar to those in the wild type (Normanly et al., 1997). Additionally, the *nit1-3* allele does not suppress the auxin accumulation phenotype of *sur2-1* in a double mutant (Bak et al., 2001), and incorporation of label into IAN or from IAN to IAA was not observed in labeling studies of *sur2-1* (Barlier et al., 2000). These attempts to validate a role for *NIT1* and IAN in IAA synthesis have not yielded definitive results. *NIT1* is a member of a gene family with overlapping expression patterns in the root, and this redundancy has generally made it difficult to assess the role of IAN and nitrilases in IAA synthesis. Combinations of mutants (e.g., a *cyp79B2 cyp79B3 nit* triple mutant or a multiple nitrilase mutant) could be more informative.

Our results suggest redundancy in the IAA synthesis pathways and enzymes involved in root IAA biosynthesis. Specifically, the CYP79B2 and CYP79B3 enzymes appear to be involved, although it remains to be determined how IAOx is converted to IAA. It has also been observed that wounding stimulates Trp-dependent synthesis. Sztein et al. (2002) showed that Trp-dependent IAA synthesis was predominant in tissue distal to a wound site immediately after wounding and much less so at 36 and 120 h after wounding. For our experiments with excised roots, we analyzed tissue distal to the wound site at 24 h after excision, so we cannot exclude the possibility that an alternative Trp-dependent IAA is specifically upregulated in the excised roots of the *cyp79B2 cyp79B3* double mutant, thereby partially masking the significance of the CYP79B2 and CYP79B3 enzymes in root IAA synthesis. To get a more complete picture of the upstream and downstream events of IAA synthesis, it would be of great interest to be able to measure the levels and synthesis rates of different IAA precursors, catabolites, and conjugates in

specific root tissues. This would make it possible to monitor the metabolic flow through the pathways more accurately, both to estimate their relative importance and to localize tissues that function as auxin sinks in the root.

METHODS

Plant Material and Growth Conditions

Seeds from wild-type *Arabidopsis thaliana* ecotype Columbia were sterilized, plated on solid medium (1× MS medium, 1% sucrose, and 0.7% agar, pH 5.7), and cold treated for 3 d to break dormancy and synchronize germination. MS medium was from Duchefa (Haarlem, The Netherlands), and agar (Agar-agar) was from Merck (Darmstadt, Germany). After cold treatment, the plates were placed vertically under long-day conditions (16 h of light, 8 h of darkness) at a temperature of 22°C. The Arabidopsis lines *tir7-1*, *sur2-1*, *sur1-3*, *nit1-3*, and the *cyp79B2 cyp79B3* double mutant were grown under the same conditions as the wild type. These lines are all in the Columbia background. Homozygous seedlings of the mutant *sur1-3* were selected from plates before incubation in medium containing ^2H_2O.

Roots from wild-type seedlings were collected at 3, 4, 7, and 8 DAG, cleared according to Malamy and Benfey (1997), and mounted in 50% glycerol on microscope slides. Root length was measured and lateral roots were counted and classified (Malamy and Benfey, 1997) using a Leica MZFL III stereomicroscope (Leica Microscopy Systems, Heerbrugg, Switzerland).

Characterization of the *tir7-1* Mutant

The root wave phenotype of the *tir7-1* mutant was scored as described by Rutherford et al. (1998). To determine the sequence of *ASA1* in *tir7-1*, fragments of the gene were amplified by PCR and sequenced directly. At least two independent PCR procedures were used for each primer pair.

GUS Constructs

CYP79B2-GUS was constructed by subcloning into the *Bam*HI site of pBI101.2 a genomic fragment of *CYP79B2* (At4g39950) beginning at an artificial *Bam*HI site approximately −6000 from the initiation codon and extending to a *Bam*HI site located at +141 from the initiation codon of *CYP79B2*. *CYP79B3-GUS* was constructed by subcloning into the *Hin*dIII and *Sal*I sites of pBI101.2 a genomic fragment of *CYP79B3* (At2g22330) beginning at an artificial *Sal*I site approximately −5200 from the initiation codon and extending to an artificial *Hin*dIII site located at +141 from the initiation codon. Transformation of plants was done by floral dip, and transgenic plants were selected on PNS medium (Haughn and Somerville, 1986) without sucrose containing kanamycin (15 μg/mL). Four transgenic lines that showed similar staining patterns were analyzed for each reporter. Reporter constructs were grown hydroponically in 3 mL of PNS at 21°C under continuous light (20 to 30 $\mu E \cdot m^{-2} \cdot s^{-1}$) in six-well culture dishes for 7 DAG. For IAA induction experiments, seedlings were grown hydroponically for 7 DAG, after which IAA was added to the medium (final concentration, 1 μM) and plants were grown for an additional 24 h.

GUS activity was detected in whole plants as follows. The plants were submerged in 2 to 3 mL of GUS buffer (0.1 M sodium phosphate, pH 7.0, 0.5 mM potassium ferricyanide, 0.5 mM potassium ferrocyanide, 10 mM EDTA, 0.01% Triton X-100, and 0.2 mg/mL X-Gluc [Rose Scientific, Edmonton, Canada] dissolved in 50 to 100 μL of dimethylformamide and filtered through a 45-μm filter) (Jefferson, 1987) and incubated at 37°C in the dark for 1 h (*CYP79B2-GUS*) or 18 h (*CYP79B3-GUS*). Stained plants were washed once in sterile water and then destained in several changes of 70% ethanol until the chlorophyll was bleached. The plants were stored in 50% glycerol with 0.01% Triton X-100. Photographs representative of each line were taken using a Nikon (Melville, NY) E600 phase contrast microscope with a Pixera (Los Gatos, CA) camera and software or on a Leica MZ6 dissecting microscope with a 35-mm camera.

^2H_2O Feedings

Three- and 7-d-old wild-type Arabidopsis Columbia seedlings were transferred to Petri dishes with liquid medium (1× MS medium and 1% sucrose, pH 5.7) containing ^2H_2O ($^2H_2$ = 70%; Cambridge Isotope Laboratories, Andover, MA). Four different treatments were applied: intact seedlings were incubated in medium containing 30% ^2H_2O or 30% ^2H_2O and 40 μM NPA, and whole roots cut at the hypocotyl–root junction (excised roots) were incubated in medium containing 30% ^2H_2O or 30% ^2H_2O and 40 μM NPA. All seedlings were incubated for 24 h in long-day conditions with gentle shaking. After incubation, seedlings and roots were rinsed in distilled water and the roots were dissected on a stereomicroscope. The root tip or whole root was sectioned in 0.5-, 2-, or 8-mm sections. For each sample, 100, 50 to 100, or 25 root sections (equivalent to 0.5 to 2 mg of tissue), respectively, were pooled in 1.5-mL microcentrifuge tubes containing 50 μL of cold extraction buffer. For collection of lateral root tips, 10-d-old seedling roots cut at the hypocotyl–root junction were incubated for 24 h in medium containing 30% ^2H_2O. The apical 2 mm part of developing lateral roots was collected (100 sections per sample). The samples were frozen in liquid nitrogen and stored at −80°C until extraction and purification. All samples were collected in triplicate.

Arabidopsis mutant seedlings (intact seedlings or excised roots) were incubated at 7 DAG for 24 h in liquid medium (1× MS medium and 1% sucrose, pH 5.7) containing 30% ^2H_2O. Wild-type Columbia seedlings treated and incubated in the same way were used as controls. The most apical (closest to the root tip) 4 mm of the root was collected and divided into 2-mm sections. Fifty to 100 sections were pooled for each sample. All samples were collected in triplicate.

For comparison between different analytical methods (HR-SIM and SRM-MS), 10-d-old seedlings were incubated in liquid medium containing ^2H_2O for 12 or 24 h. Three different treatments were made: intact seedlings were incubated in medium containing 30% ^2H_2O or 30% ^2H_2O and 40 μM NPA, and excised roots were incubated in medium containing 30% ^2H_2O. Sample weight was 30.1 ± 9.6 mg, and whole roots from 10 seedlings were pooled for each sample. The samples were collected in triplicate.

IAA and IAN Quantification and Biosynthesis Measurements

Samples containing larger amounts of plant material (30 mg) were homogenized, extracted, and purified as described by Edlund et al. (1995) with the addition of an extra purification step. After purification on XAD-7, the sample was methylated with diazomethane, evaporated to dryness, dissolved in 1% acetic acid containing 10% methanol, and applied to a 50-mg C18 BondElut SPE column (Varian, Middelburg, The Netherlands) (conditioned with 1 mL of methanol and 1 mL of 1% acetic acid). The column was washed with 1 mL of 20% methanol in 1% acetic acid. IAN and methylated IAA were then eluted with 1 mL of methanol, evaporated to dryness, and trimethylsilylated as described by Edlund et al. (1995). Samples containing small amounts of root tissue (0.5 to 2 mg) were homogenized and extracted as described by Edlund et al. (1995). The pH of the sample was adjusted to 2.7, and the sample was purified directly on a 50-mg C18 BondElut SPE column as described above, thus excluding the XAD-7 step. The sample was then methylated and trimethylsilylated.

After derivatization, the sample was dissolved in 15 μL of *n*-heptane and injected with a HP 7683 Series autoinjector into a HP 6890 Series gas chromatograph (Agilent Technologies, Palo Alto, CA) equipped with a

30-m × 0.25-mm i.d. analytical GC column with a 0.25-μm CP-Sil 8 CB-MS stationary phase (Chrompack; Varian). The injection temperature was 260°C, and samples were eluted with the following GC temperature program: 80°C for 2 min, 20°C/min up to 200°C, 4°C/min up to 220°C, and finally 30°C/min up to 260°C. The mass spectrometer was a JMS-700 MStation double-focusing magnetic sector instrument (JEOL, Tokyo, Japan), and analysis was performed either by GC-HR-SIM-MS or GC-SRM-MS using pentafluorokerosene as calibration substance.

In HR-SIM mode, the isotopomers of the base peak of IAA-Me-TMS with m/z values of 202.105, 203.112, 204.118, and 205.124 were used as diagnostic ions for the incorporation of deuterium atoms into the IAA molecule, and m/z 208.125 from [$^{13}C_6$]IAA-Me-TMS was also recorded. The measurements were performed at a resolution of 10,000 using accelerating voltage switching from 10 kV and a dwell time of 50 ms. Pentafluorokerosene m/z 192.989 was used as lock mass.

SRM measurements of IAA and IAN biosynthesis rates were performed with an acceleration voltage of 10 kV. The metastable precursor ions were selected by magnetic switching, and daughter ions formed in the first field-free region were detected by simultaneous switching of the magnetic and electrostatic fields. The dwell time was 100 ms. No collision gas was used. For IAA, the reactions m/z 261.118 to 202.105, m/z 262.125 to 203.112, m/z 263.131 to 204.118, m/z 264.137 to 205.124, and m/z 267.137 to 208.125 were recorded. Corrections were made for the contribution of natural isotopic abundances to m/z 203 to 205 using the diagnostic ions of standard [$^{12}C_6$]IAA-Me-TMS. The incorporation of deuterium into the IAA molecule was then calculated, and corrections for background in the samples were made by analyzing control samples incubated without ^2H_2O. IAN was analyzed as the trimethylsilyl derivative in the SRM mode, using the metastable transitions m/z 228.108 to 213.085, m/z 229.115 to 214.091, m/z 230.121 to 215.097, and m/z 231.127 to 216.103. Corrections were made for the contribution of natural isotopic abundances to m/z 214 to 216 using the diagnostic ions of standard [$^{12}C_6$]IAN-TMS. The incorporation of deuterium into the IAN molecule was then calculated, and corrections for background were made by analyzing control samples incubated without ^2H_2O.

The amount of endogenous IAA in the samples was quantified by combining the corrected areas of the ions from deuterium-labeled IAA (m/z 203 to 205) with that of unlabeled IAA (m/z 202). The calculation of isotopic dilution was based on the addition of 100 to 250 pg of [$^{13}C_6$]IAA (Cambridge Isotope Laboratories) per sample. Because of the lack of a suitable internal standard for IAN, it was not possible to quantify this substance. Synthesis rates of IAA and IAN in wild-type versus mutant seedlings were compared using Student's *t* test (two-sample assuming equal variances, two-tailed distribution).

Sequence data from this article have been previously deposited with the EMBL/GenBank data libraries under accession numbers NM_120158 (CYP79B2) and NM_127798 (CYP79B3).

ACKNOWLEDGMENTS

We thank Roger Granbom and Gun Löfdahl for excellent technical assistance. This research was funded by grants from the Swedish Research Council and the Swedish Foundation for Strategic Research to G.S., by National Science Foundation Grant DBI-0077769 and USDA Grant 2002-35318-12715 to J.N. and J.C., and by National Institutes of Health Grant GM-43644 and U.S. Department of Energy Grant DE-FG02-02ER15312 to M.E. Seeds were kind gifts from Catherine Bellini (*sur1-3* and *sur2-1*) and Bonnie Bartel (*nit1-3*). We also thank Malcolm Bennett for helpful comments on the manuscript.

Received November 12, 2004; accepted January 18, 2005.

REFERENCES

Åstot, C., Dolezal, K., Moritz, T., and Sandberg, G. (2000). Deuterium in vivo labelling of cytokinins in *Arabidopsis thaliana* analysed by capillary liquid chromatography/frit-fast atom bombardment mass spectrometry. J. Mass Spectrom. **35,** 13–22.

Bak, S., Tax, F.E., Feldmann, K.A., Galbraith, D.W., and Feyereisen, R. (2001). CYP83B1, a cytochrome P450 at the metabolic branch point in auxin and indole glucosinolate biosynthesis in Arabidopsis. Plant Cell **13,** 101–111.

Barlier, I., Kowalczyk, M., Marchant, A., Ljung, K., Bhalerao, R., Bennett, M., Sandberg, G., and Bellini, C. (2000). The *SUR2* gene of *Arabidopsis thaliana* encodes the cytochrome P450 CYP83B1, a modulator of auxin homeostasis. Proc. Natl. Acad. Sci. USA **97,** 14819–14824.

Bartel, B., and Fink, G.R. (1994). Differential regulation of an auxin-producing nitrilase gene family in *Arabidopsis thaliana*. Proc. Natl. Acad. Sci. USA **91,** 6649–6653.

Bartel, B., LeClere, S., Magidin, M., and Zolman, B.K. (2001). Inputs to the active indole-3-acetic acid pool: De novo synthesis, conjugate hydrolysis, and indole-3-butyric acid β-oxidation. J. Plant Growth Regul. **20,** 198–216.

Bauerle, R., Hess, J., and French, S. (1987). Anthranilate synthase-anthranilate phosphoribosyltransferase complex and subunits of *Salmonella typhimurium*. Methods Enzymol. **142,** 366–386.

Beeckman, T., Burssens, S., and Inze, D. (2001). The peri-cell-cycle in *Arabidopsis*. J. Exp. Bot. **52,** 403–411.

Bender, J., and Fink, G.R. (1998). A Myb homologue, ATR1, activates tryptophan gene expression in *Arabidopsis*. Proc. Natl. Acad. Sci. USA **95,** 5655–5660.

Benfey, P.N., and Scheres, B. (2000). Root development. Curr. Biol. **16,** R813–R815.

Benková, E., Michniewicz, M., Sauer, M., Teichmann, T., Seifertová, D., Jürgens, G., and Friml, J. (2003). Local, efflux-dependent auxin gradients as a common module for plant organ formation. Cell **115,** 591–602.

Bhalerao, R.P., Eklöf, J., Ljung, K., Marchant, A., Bennett, M., and Sandberg, G. (2002). Shoot derived auxin is essential for early lateral root emergence in *Arabidopsis* seedlings. Plant J. **29,** 325–332.

Bialek, K., Michalczuk, L., and Cohen, J.D. (1992). Auxin biosynthesis during seed germination in *Phaseolus vulgaris*. Plant Physiol. **100,** 509–517.

Birnbaum, K., Shasha, D.E., Wang, J.Y., Jung, J.W., Lambert, G.M., Galbraith, D.W., and Benfey, P.N. (2003). A gene expression map of the *Arabidopsis* root. Science **302,** 1956–1960.

Boerjan, W., Cervera, M.-T., Delarue, M., Beeckman, T., Dewitte, W., Bellini, C., Caboche, M., Van Onckelen, H., Van Montagu, M. and Inzé, D. (1995). *superroot*, a recessive mutation in Arabidopsis, confers auxin overproduction. Plant Cell **7,** 1405–1419.

Boros, L., Cascante, M., and Lee, W.-N. (2003). Stable isotope-based dynamic metabolic profiling in disease and health. In Metabolic Profiling: Its Role in Biomarker Discovery and Gene Function Analysis, G. Harrigan and R. Goodacre, eds (Boston: Kluwer Academic Publishers), pp. 141–169.

Casimiro, I., Beeckman, T., Graham, N., Bhalerao, R., Zhang, H., Casero, P., Sandberg, G., and Bennett, M.J. (2003). Dissecting *Arabidopsis* lateral root development. Trends Plant Sci. **4,** 165–171.

Casimiro, I., Marchant, A., Bhalerao, R.P., Beeckman, T., Dhooge, S., Swarup, R., Graham, N., Inzé, D., Sandberg, G., Casero, P.J., and Bennett, M. (2001). Auxin transport promotes Arabidopsis lateral root initiation. Plant Cell **13,** 843–852.

Celenza, J.L., Quiel, J.A., Smolen, G.A., Merrikh, H., Silvestro, A., Normanly, J., and Bender, J. (2005). The Arabidopsis ATR1 Myb

transcription factor controls indolic glusocinolate homeostasis. Plant Physiol. **137,** 253–262.

Chapman, J.R. (1993). Selected reaction monitoring. In Practical Organic Mass Spectrometry: A Guide for Chemical and Biochemical Analysis, 2nd ed. (Chichester, UK: John Wiley & Sons), pp. 292–297.

Cooney, T.P., and Nonhebel, H.M. (1991). Biosynthesis of indole-3-acetic acid in tomato shoots: Measurement, mass-spectral identification and incorporation of ^2H from ^2H_2O into indole-3-acetic acid, D- and L-tryptophan, indole-3-pyruvate and tryptamine. Planta **184,** 368–376.

Dolan, L., and Davies, J. (2004). Cell expansion in roots. Curr. Opin. Plant Biol. **7,** 33–39.

Edlund, A., Eklöf, S., Sundberg, B., Moritz, T., and Sandberg, G. (1995). A microscale technique for gas-chromatography mass-spectrometry measurements of picogram amounts of indole-3-acetic acid in plant tissues. Plant Physiol. **108,** 1043–1047.

Friml, J. (2003). Auxin transport: Shaping the plant. Curr. Opin. Plant Biol. **6,** 7–12.

Friml, J., Benková, E., Blilou, I., Wisniewska, J., Hamann, T., Ljung, K., Woody, S., Sandberg, G., Scheres, B., Jürgens, G., and Palme, K. (2002a). AtPIN4 mediates sink-driven auxin gradients for root patterning in *Arabidopsis*. Cell **108,** 661–673.

Friml, J., Wisniewska, J., Benkova, E., Mendgen, K., and Palme, K. (2002b). Lateral relocation of auxin efflux regulator PIN3 mediates tropisms in *Arabidopsis*. Nature **415,** 806–809.

Gaskell, S.J., and Millington, D.S. (1978). Selected metastable peak monitoring: A new, specific technique in quantitative gas chromatography mass spectrometry. Biomed. Mass Spectrom. **5,** 557–558.

Grebe, M. (2004). Ups and downs of tissue and planar polarity in plants. Bioessays **26,** 719–729.

Haughn, G.W., and Somerville, C. (1986). Sulfonylurea-resistant mutants of *Arabidopsis thaliana*. Mol. Gen. Genet. **204,** 430–434.

Hillebrand, H., Bartling, D., and Weiler, E.W. (1998). Structural and functional analysis of the *nit2/nit1/nit3* gene cluster encoding nitrilases, enzymes catalyzing the terminal activation step in indole-acetic acid biosynthesis in *Arabidopsis thaliana*. Plant Mol. Biol. **36,** 89–99.

Hull, A.K., Vij, R., and Celenza, J.L. (2000). *Arabidopsis* cytochrome P450s that catalyze the first step of tryptophan-dependent indole-3-acetic acid biosynthesis. Proc. Natl. Acad. Sci. USA **97,** 2379–2384.

Jefferson, R.A. (1987). Assaying chimeric genes in plants: The GUS gene fusion system. Plant Mol. Biol. Reporter **5,** 387–405.

Jensen, P.J., and Bandurski, R.S. (1996). Incorporation of deuterium into indole-3-acetic acid and tryptophan in *Zea mays* seedlings grown on 30% deuterium oxide. J. Plant Physiol. **147,** 697–702.

Kushner, D.J., Baker, A., and Dunstall, T.G. (1998). Pharmacological uses and perspectives of heavy water and deuterated compounds. Can. J. Physiol. Pharmacol. **77,** 79–88.

Kutz, A., Müller, A., Hennig, P., Kaiser, W.M., Piotrowski, M., and Weiler, E.W. (2002). A role for nitrilase 3 in the regulation of root morphology in sulphur-starving *Arabidopsis thaliana*. Plant J. **30,** 95–106.

Laskowski, M.J., Williams, M.E., Nusbaum, C., and Sussex, I.M. (1995). Formation of lateral root meristems is a two-stage process. Development **121,** 3303–3310.

Ljung, K., Bhalerao, R.P., and Sandberg, G. (2001). Sites and homeostatic control of auxin biosynthesis in *Arabidopsis* during vegetative growth. Plant J. **28,** 465–474.

Ljung, K., Hull, A.K., Kowalczyk, M., Marchant, A., Celenza, J., Cohen, J.D., and Sandberg, G. (2002). Biosynthesis, conjugation, catabolism and homeostasis of indole-3-acetic acid in *Arabidopsis thaliana*. Plant Mol. Biol. **50,** 309–332.

Malamy, J.E., and Benfey, P.N. (1997). Organization and cell differentiation in lateral roots of *Arabidopsis thaliana*. Development **124,** 33–44.

Marchant, A., Bhalerao, R.P., Casimiro, I., Eklöf, J., Casero, P.J., Bennett, M., and Sandberg, G. (2002). AUX1 promotes lateral root formation by facilitating IAA distribution between sink and source tissues in the Arabidopsis seedling. Plant Cell **14,** 589–597.

Mikkelsen, M.D., Hansen, C.H., Wittstock, U., and Halkier, B.A. (2000). Cytochrome P450 CYP79B2 from *Arabidopsis* catalyzes the conversion of tryptophan to indole-3-acetaldoxime, a precursor of indole glucosinolates and indole-3-acetic acid. J. Biol. Chem. **275,** 33712–33717.

Mikkelsen, M.D., Naur, P., and Halkier, B.A. (2004). *Arabidopsis* mutants in the C-S lyase of glucosinolate biosynthesis establish a critical role for indole-3-acetaldoxime in auxin homeostasis. Plant J. **37,** 770–777.

Mizutani, M., Ward, E., and Ohta, E. (1998). Cytochrome P450 superfamily in *Arabidopsis thaliana*: Isolation of cDNAs, differential expression, and RFLP mapping of multiple cytochromes P450. Plant Mol. Biol. **37,** 39–52.

Moritz, T. (1996). Mass spectrometry of plant hormones. In Applications of Modern Mass Spectrometry in Plant Science Research, R.P. Newton and T.J. Walton, eds (Oxford, UK: Clarendon Press), pp. 139–158.

Moritz, T., and Olsen, J.E. (1995). Comparison between high-resolution selected ion monitoring, selected reaction monitoring, and four-sector tandem mass spectrometry in quantitative analysis of gibberellins in milligram amounts of plant tissue. Anal. Chem. **67,** 1711–1716.

Muday, G. (2001). Auxins and tropisms. J. Plant Growth Regul. **20,** 226–243.

Müller, A., Hillebrand, H., and Weiler, E.W. (1998). Indole-3-acetic acid is synthesized from L-tryptophan in roots of *Arabidopsis thaliana*. Planta **206,** 362–369.

Niyogi, K.K. (1993). Molecular and Genetic Analysis of Anthranilate Synthase in *Arabidopsis thaliana*. PhD dissertation (Cambridge, MA: Massachusetts Institute of Technology).

Niyogi, K.K., and Fink, G.R. (1992). Two anthranilate synthase genes in Arabidopsis: Defense-related regulation of the tryptophan pathway. Plant Cell **4,** 721–733.

Normanly, J., Grisalfi, P., Fink, G., and Bartel, B. (1997). Arabidopsis mutants resistant to the auxin effects of indole-3-acetonitrile are defective in the nitrilase encoded by the NIT1 gene. Plant Cell **9,** 1781–1790.

Normanly, J., Slovin, J.P., and Cohen, J.D. (2005). Auxin biosynthesis and metabolism. In Plant Hormones: Biosynthesis, Signal Transduction, Action! 3rd ed. P.J. Davies, ed (Dordrecht, The Netherlands: Kluwer Academic Publishers), pp. 36–62.

Ottenschläger, I., Wolff, P., Wolverton, C., Bhalerao, R.P., Sandberg, G., Ishikawa, H., Evans, M., and Palme, K. (2003). Gravity-regulated differential auxin transport from columella to lateral root cap cells. Proc. Natl. Acad. Sci. USA **100,** 2987–2991.

Peer, W.A., Bandyopadhyay, A., Blakeslee, J.J., Makam, S.N., Chen, R.J., Masson, P.H., and Murphy, A.S. (2004). Variation in expression and protein localization of the PIN family of auxin efflux facilitator proteins in flavonoid mutants with altered auxin transport in *Arabidopsis thaliana*. Plant Cell **16,** 1898–1911.

Pruitt, K.D., and Last, R.L. (1993). Expression patterns of duplicate tryptophan synthase β genes in *Arabidopsis thaliana*. Plant Physiol. **102,** 1019–1026.

Rashotte, A., Brady, S.R., Reed, R.C., Ante, S.J., and Muday, G.M. (2000). Basipetal auxin transport is required for gravitropism in roots of Arabidopsis. Plant Physiol. **122,** 481–490.

Ruegger, M., Dewey, E., Hobbie, L., Brown, D., Bernasconi, P., Turner, J., Muday, G., and Estelle, M. (1997). Reduced NPA-binding

in the *tir3* mutant of Arabidopsis is associated with a reduction in polar auxin transport and diverse morphological defects. Plant Cell **9,** 745–757.

Rutherford, R., Gallois, P., and Masson, P.H. (1998). Mutations in *Arabidopsis thaliana* genes involved in the tryptophan biosynthesis pathway affect root waving on tilted agar surfaces. Plant J. **16,** 145–154.

Schiefelbein, J.W., and Benfey, P.N. (1994). Root development in *Arabidopsis*. In Arabidopsis, E.M. Meyerowitz and C.R. Somerville, eds. (Cold Spring Harbor, NY: Cold Spring Harbor Laboratory Press), pp. 335–353.

Sekimoto, H., Seo, M., Kawakami, N., Komano, T., Desloire, S., Liotenberg, S., Marion-Poll, A., Caboche, M., Kamiya, Y., and Koshiba, T. (1998). Molecular cloning and characterization of aldehyde oxidases in *Arabidopsis thaliana*. Plant Cell Physiol. **39,** 433–442.

Smolen, G., and Bender, J. (2002). *Arabidopsis* cytochrome P450 *cyp83B1* mutations activate the tryptophan biosynthetic pathway. Genetics **160,** 323–332.

Swarup, R., Friml, J., Marchant, A., Ljung, K., Sandberg, G., Palme, K., and Bennett, M. (2001). Localization of the auxin permease AUX1 suggests two functionally distinct hormone transport pathways operate in the *Arabidopsis* root apex. Genes Dev. **15,** 2648–2653.

Sztein, A.E., Ilic, N., Cohen, J.D., and Cooke, T.J. (2002). Indole-3-acetic acid biosynthesis in isolated axes from germinating bean seeds: The effect of wounding on the biosynthetic pathway. Plant Growth Regul. **36,** 201–207.

Thorne, G.C., and Gaskell, S.J. (1985). Dual metastable peak monitoring: Application to the analysis of oestradiol-17β as the bis (tert-butyldimethylsilyl) ether. Biomed. Mass Spectrom. **12,** 19–24.

van der Weele, C.M., Jiang, H.S., Palaniappan, K.K., Ivanov, V., Palaniappan, K., and Baskin, T. (2003). A new algorithm for computational image analysis of deformable motion at high spatial and temporal resolution applied to root growth: Roughly uniform elongation in the meristem and also, after an abrupt acceleration, in the elongation zone. Plant Physiol. **132,** 1138–1148.

Vorwerk, S., Biernacki, S., Hillebrand, H., Janzki, I., Muller, A., and Weiler, E.W. (2001). Enzymatic characterization of the recombinant *Arabidopsis thaliana* nitrilase subfamily encoded by the NIT2/NIT1/NIT3 gene cluster. Planta **212,** 508–516.

Zhao, Y., Hull, A.K., Gupta, N.R., Goss, K.A., Alonso, J., Ecker, J.R., Normanly, J., Chory, J., and Celenza, J.L. (2002). Trp-dependent auxin biosynthesis in *Arabidopsis*: Involvement of cytochrome P450s CYP79B2 and CYP79B3. Genes Dev. **16,** 3100–3112.